Multiscale and Multidisciplinary Modeling, Experiments and Design (2024) 7:787–800
https://doi.org/10.1007/s41939-023-00245-x

ORIGINAL RESEARCH

Effects of slag and zeolite on mechanical properties and durability of rapid strengthening ultra-high-performance concrete

Ataollah Hajati Modaraei[1] · **Bijan Bijan**[1]

Accepted: 4 September 2023 / Published online: 4 October 2023

Abstract
Rapid strengthening ultra-high-performance concretes (RS-UHPCs) have great potential in repair applications and precast elements manufacturing. Using industrial and natural pozzolans to reduce cement consumption and carbon dioxide footprint can be a crucial step in the industrial and economic development of UHPCs. In this study, by introducing ten mix designs based on UHPC and replacing 5%, 10%, and 15% by weight of silica fume with single pozzolans including slag and zeolite separately and a combination of percentages of both pozzolans as a silica fume replacement up to 15% by weight, various tests, including evolutions in internal temperature, setting time, compressive strength, and electrical resistivity in early and higher ages and final water absorption were performed on the specimens. The test results revealed that each of the pozzolans exhibits a different behavior during the hardening period, early and higher ages. In addition, a strong mathematical correlation was found between the results of various mechanical and durability tests. Slag and zeolite in amount of 5% cement weight in the mix designs, acquired the best results in terms of mechanical and durability properties, and percentages of 15% in single and complex conditions gave relatively lower results. The microstructural evaluation of the two optimal designs showed the increased compaction and improved C.S.H. growth due to pozzolan replacement with silica fume.

Keywords Ultra-high-performance concrete · Zeolite · Slag · Electrical resistivity · Hydration heat

1 Introduction

Using admixtures such as fibers and mineral fillers to improve the mechanical properties of cementitious composites has been studied and industrialized during the past decades (Ahmad et al. 2022; Jan et al. 2022; Moein et al. 2019). In recent years, tremendous improvements have been reached in the development of UHPC technology (Bahmani and Mostofinejad 2022; Du et al. 2021; Sharma et al. 2022; Wang et al. 2021). Nowadays, this type of concrete is used as a standard construction material with a compressive strength of at least 120 MPa in the industry (ASTM 2017). Achieving ultra-high performance at an early age is a crucial step for UHPC. Due to this property of UHPC, this type of concrete for structural purposes requires relatively faster and more precise operations compared to ordinary concrete, with a unique advantage. Gaining the desired mechanical strength for the structural concrete elements within 1–3 days or even less from this material investigated in numerous studies (Stein et al. 2010; United States Department of Transportation 2002).

The acquirement of mineral rock powders to improve mechanical properties of new class of cementitious composites such as high performance and ultra-high-performance concretes with the obvious environmental and economic advantages, has been the subjects of numerous research cases (Ahmad et al. 2022; Shaukat et al. 2020). The primary purpose of introducing natural zeolite (NZ) and slag in concrete mixtures is the potential of these pozzolans to improve their mechanical properties (Caputo et al. 2008; Hajforoush et al. 2019; Moein and Soliman 2022; Moein et al. 2023a; Sadrmomtazi et al. 2019; Tahmouresi et al. 2021). Recent studies show that the use of NZ in pozzolanic concretes has positive effects and a good impact on the durability and mechanical properties (Ahmadi and Shekarchi 2010; Chan and Ji 1999; Poon et al. 1999). The use of NZ in UHPC caused a significant

✉ Bijan Bijan
bijanbijannesaz@gmail.com

Ataollah Hajati Modaraei
dr.modaraei@gmail.com

[1] Department of Civil Engineering, University of Guilan, Rasht, Iran

change in the characteristics of this type of concrete while reducing cement consumption (Pezeshkian et al. 2020, 2021). In the scope of this study, as mentioned in the case of NZ, similar effects of ground granulated blast furnace slag (GGBFS) on hydration temperature, strength, and microstructural properties of UHPC observed (Kim et al. 2016; Shi et al. 2015; Xiao et al. 2014). In terms of heat evolution during hydration, UHPC can undergo significant changes due to its high cement and low water content (Sbia et al. 2017; Yalçınkaya and Çopuroğlu 2021). In this case, the necessity of using pozzolanic materials by researchers to reduce the amount of Portland cement to control the heat of hydration with the desired limits has been investigated (Bajaber and Hakeem 2021). In different studies is stated that GGBFS does not play an influential role in reducing the heat of hydration in hot climates (Kim et al. 2016; Woo et al. 2018). According to some researches, the difference of strength growth depending on the replacement ratio of GGBFS as an active pozzolan with cementitious properties to Portland cement is significant in the early curing ages (Yazici et al. 2010; Yu et al. 2014).

In various studies, a theoretical basis for realizing the relationship between hardening properties and the development of electrical resistivity is implied (Cosoli et al. 2020; Wei and Xiao 2013). This characteristic of concrete depends on the microstructure of the cement paste and the different geometries of pores, which is determined by the volume, size, and connection of them (Gholhaki et al. 2018; Mansoori et al. 2020; Moein et al. 2022, 2023b; Mosavinejad et al. 2018; Rahmati et al. 2022; Sadrmomtazi et al. 2018; Saradar et al. 2018, 2020; Shadmani et al. 2018). The electrical resistivity of concrete also depends on its moisture content and chemical structure (Gorzelańczyk and Hoła 2011; Sengul 2012). In addition, the amount of additives such as GGBFS, fly ash, and silica fume reduces the size and volume of the pores. UHPC is known as a composite with a well-packed structure and low permeability. A high degree of packing and low porosity content significantly reduces the transfer of ions through the matrix and in turn, improves the durability properties (Li et al. 2020; Wang et al. 2019).

Despite the variety and number of researches on the electrical resistivity of hardened concrete, very few specially focused studies are found in the field of UHPCs, and few studies showed a significant effect of pozzolans on electrical resistivity, specifically at higher ages (Ghasemzadeh Mosavinejad et al. 2020). Development of research and collection of laboratory data in the field of electrical resistivity of pozzolanic UHPCs can play an essential role in the comprehensive evaluation of the long-term behavior of these concretes and the application of this non-destructive method leads to the prediction of durability and mechanical properties even after several decades of UHPC's life cycle.

In this study, the effects of Zeolite and slag as a replacement of silica fume investigated on the behavior of fresh concrete by evaluating the setting time and temperature evolution of fresh concrete in the first 28 h. These pozzolans are well-known as secondary binders with relatively low pozzolanic reaction compared to silica fume which is beneficial in controlling the C.S.H. evolution of high strength cementitious composites, such as UHPC. In a matter of setting time control for rapid repair cases, such as pavements of highways with high traffic load and time sensitive projects, the modification of mix design is crucial. Moreover, in cold regions, rapid strengthening formulas specially in the case of UHPC could benefit the mediators such as zeolite to overcome drawbacks in terms of physical and mechanical properties of such concretes at the long-term performance. Furthermore, after hardening of the UHPC, by studying the mechanical properties, durability, and microstructure of these concretes, the effect of these additives for higher ages was evaluated.

2 Experimental program

2.1 Materials

The powder materials used in this research, including type II cement, were used following the specifications of the ASTM-C150 standard (ASTM 2019). Silica fume compatible with ASTM-C1240 standard specifications (ASTM 2020) was selected. GGBFS and zeolite were used to replace part of the cement up to 15% by weight, both passing through the 200 mesh sieve. The chemical characteristics of the powdered materials used are based on Table 1. In addition, silica sand passing through sieve No. 30 (less than 600 microns) was used as a fine aggregate and polycarboxylate-based superplasticizer as a water-reducing agent in accordance with ASTM C-494 (ASTM 2013). The accelerator used was powdered sodium aluminate with a purity of 98%.

2.2 Fabrication and curing

Fabrication, molding, and curing were performed following the requirements of the ASTM C109 test method (ASTM 2005) with the following changes: to make a fresh mixture, powders and silica sand were first mixed in a pan mixer to obtain a uniform dry mixture. The water and superplasticizer mixture was then gradually added over about 30 s and the mixing was continued for 1 min at 30 RPM. After that, rest around the mix pot with a spatula for 1 min to remove any unmixed material in the blades' path. Finally, for two min., mixing was continued at 60 RPM, and the mixture was ready for molding. The specimens were demolded 12 h later and the initial tests (12 h were performed on the first series of specimens, the rest of the specimens were cured under standard conditions until the determined ages. Specifications of the mix designs are presented in Table 2.

Table 1 Chemical properties of cement, silica fume, zeolite, and slag

	SiO_2	Fe_2O_3	Al_2O_3	CaO	MgO	Na_2O	K_2O	SO_3	L.O.I
Cement	22.72	2.91	3.69	62.68	4.92	0.18	0.71	2.42	1.56
Silica fume	93.4	1.14	0.64	1	0.62	–	0.03	1.14	2.9
Zeolite	69.12	0.29	12.81	2.31	1.42	2.29	1.25	0.2	8.99
GGBFS	36.6	0.52	11.1	35.4	1.7	0.6	0.82	1.02	2.1

Table 2 Mix designs (kg/m^3)

Mix code	Cement	Silica fume	GBFS	Zeolite	Water	SP	SAA
C	848	212	0	0	169.6	13.78	2.12
5G	848	159	53	0	169.6	13.78	2.12
10G	848	106	106	0	169.6	13.78	2.12
15G	848	53	159	0	169.6	13.78	2.12
5Z	848	159	0	53	169.6	13.78	2.12
10Z	848	106	0	106	169.6	13.78	2.12
15Z	848	53	0	159	169.6	13.78	2.12
5G5Z	848	106	53	53	169.6	13.78	2.12
10G5Z	848	53	106	53	169.6	13.78	2.12
5G10Z	848	53	53	106	169.6	13.78	2.12

C control mixture, *XG, YZ, XGYZ* x is the percentage of replacement of silica fume with slag, *Y* is the percentage of replacement of silica fume with zeolite

2.3 Tests

2.3.1 Internal temperature evolution

In different studies, various forms of semi-adiabatic chambers used to measure the heat of hydration, heat flow and monitoring the internal temperature variations of different concretes, including UHPC (An et al. 2016; Liu et al. 2018; Soliman and Nehdi 2013; Viviani et al. 2022). In the present study, a customized 0.4 mm thick polymer spherical mold (plastic ball) was used to build the UHPC paste spherical specimens. UHPC paste (without aggregate) was made according to the mix design and poured into the mold immediately. The J-type thermocouple sensor was placed in the center of the sphere, and the fabricated specimen, including the polymer mold, was installed inside the EPS insulation box, as shown in Fig. 1, to measure the internal temperature evolution of the UHPC specimens. The temperature measurements monitored and recorded by the digital counter every 15 min. up to 28 h, and the range was reported with temperature changes due to the development of heat in the center of the specimen.

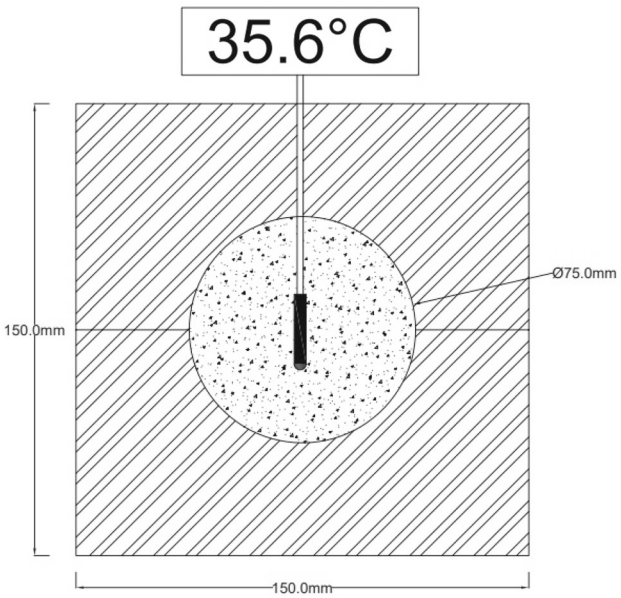

Fig. 1 Schematic diagram of measuring setup for internal temperature evolution of UHPC paste in the first 28 h after molding

2.3.2 Setting time

The paste fabricated to assess the heat evolution, also used to measure the initial and final setting time with the vicat needle device. Apart from the specifications and method of fabricating UHPC paste, the rest of the test procedure and calculations were performed according to ASTM C191 (American Society for Testing and Materials 2008).

2.3.3 Compressive and flexural strength

Compressive strength tests at the ages of 1/2, 1, 2, 7, 28, and 90 days were performed on cubic specimens with a dimension of 7.5 cm and in accordance with BS EN 12390-3 (British Standards Institution 2019). In addition, the flexural strength test according to ASTM C348 (ASTM 2021) was performed on prismatic specimens with dimensions of 4 × 4 × 16 cm.

2.3.4 Electrical resistivity and final water absorption

The electrical resistivity of the specimens was measured according to the AASHTO TP95 standard (AASHTO TP 95-11 2011) using the compressive strength specimens at the same test ages and by a pair of plate electrodes on opposite sides of the specimens. To achieve reliable results, all three specimens were tested for each mix design at every age and under saturated conditions. The final water absorption was also performed on compressive strength specimens following ASTM C642 (ASTM 2013).

2.3.5 Microstructure

UHPC microstructural evaluation has a relatively good research background, and extensive studies have been conducted so far on the effect of additives and their role in the structure formation of the cement matrix (Wang et al. 2015). Scanning electron microscopy was used to examine the microstructure of UHPC specimens containing different pozzolans. SEM images with 50 kX and 75 kX magnifications were used to evaluate the cement matrix of the specimens and the role of zeolite and slag pozzolans in the UHPC microstructure.

3 Results and discussion

3.1 Fresh state

The results of the temperature evolution testing of the pastes categorized based on mix designs in Fig. 1 show that each of the pozzolans alone or in combination has different effects on the temperature evolution of the specimens. Mixtures containing slag (Fig. 2a) reaching up to 510 min. have a temperature range close to the control design. Still, over time, and especially in the time range of 1395 min., a significant difference emerged, and the temperature growth trend at this time for the design containing Slag was much faster. The initiation of heat evolution in specimens containing slag has a delay compared to control mix design which is previously studied and confirmed (Yalçınkaya and Çopuroğlu 2021). It can be stated that slag started its slow pozzolanic activity

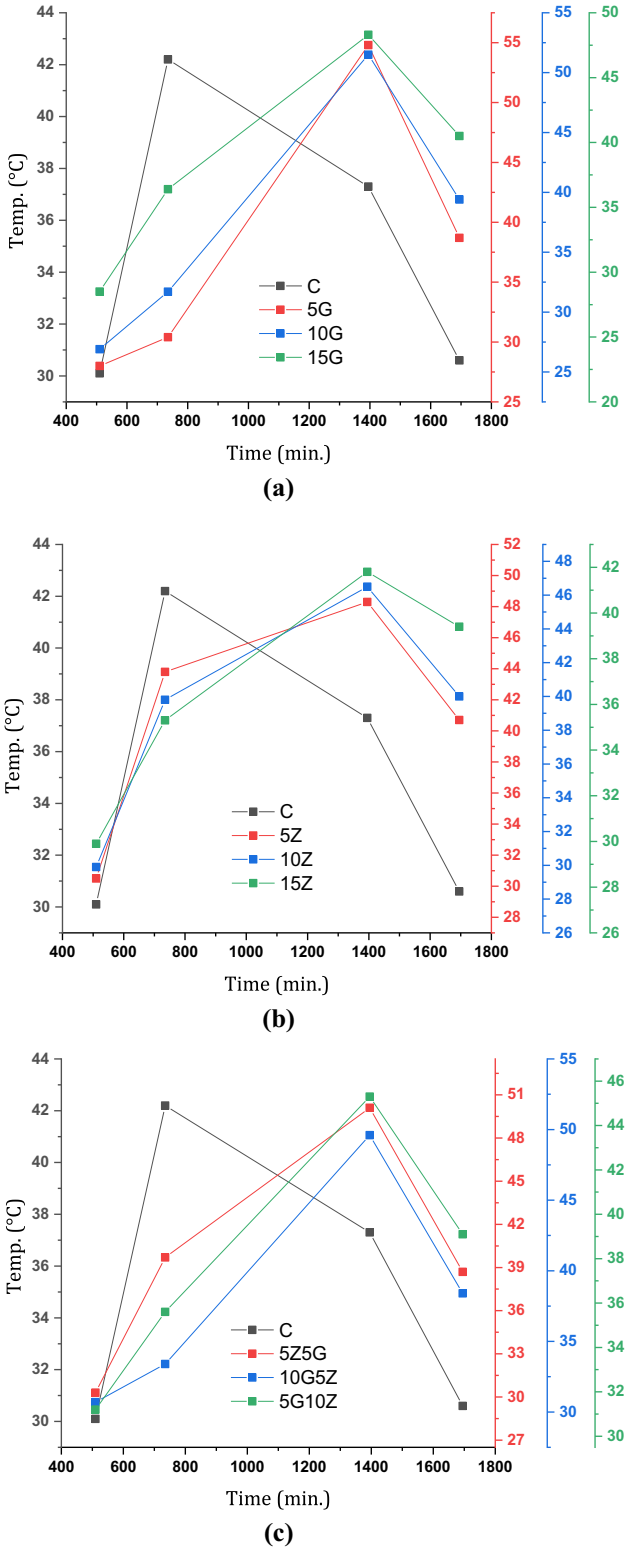

Fig. 2 Temperature evolution of the control design in the first 30 h after molding and its comparison with designs containing pozzolan. **a** Comparison of designs containing slag. **b** Comparison with designs containing zeolite. **c** Comparison with designs containing slag and zeolite simultaneously

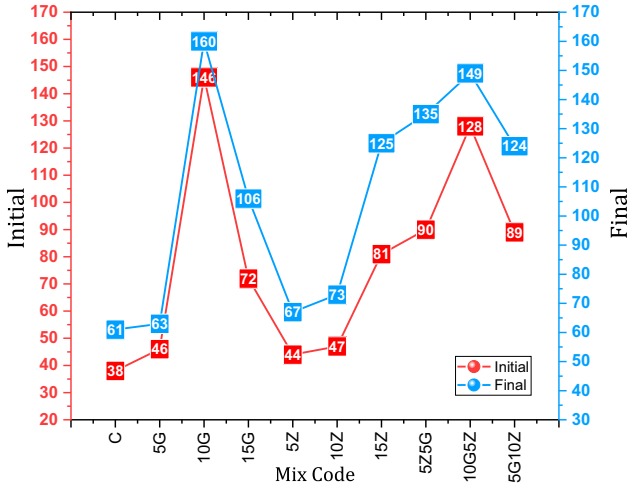

Fig. 3 Initial and final setting time of paste from different mix designs

due to the temperature jump and the presence of an accelerating agent in this time range, and the delay was probably due to slag activity and the relatively slow hydration process of secondary pozzolanic reactions so the minimum temperature increase of 46.9% (5G) is observed in this period. In contrast, the rate of temperature increase of the control mix design in the previous period (735 min.) is much higher than the mix designs containing slag. The 15G mix had the least difference from the control mix in this time period (difference of 13.7%) and the decrease observed in the next time step. This temperature jump evidently repeated in the 15G mix design due to the cementitious properties of the slag and its synergy with the cement. According to Fig. 2b, zeolite showed more activity than slag. In 735 min., the 5Z design appeared with a slight difference (3.8%) above the control design and even in 1395 min., at least The difference (15Z design compared to the control design) reached 16.3%, which was much closer to the control design than the trend of mix changes containing slag. Zeolite keeps the initial temperature rise close to the control mix which is practical in cold regions and reaching higher temperatures in mixes including high percentage of zeolite can improve the hardening process. Simultaneous use of two pozzolans of slag and zeolite in complex designs (Fig. 2c) slowed down the slag reaction to some extent and neutralized the optimum activity of zeolite and the minimum difference in thermal peak (time interval 1395 min.) reached 21.4% Which implies a difference of 5.1% compared to the previous chart data. Increasing the hydration temperature over 28 h can be helpful in slag-containing concretes, especially in cold regions and seasons, and to neutralize the slow setting due to cold weather to some extent.

Slag and zeolite pozzolans had different effects on the setting time of UHPC paste. Based on the results in Fig. 3, the most significant increase in setting time was obtained in the 10G design, which final setting took 2.62 times longer than the control design. However, this trend sharply decreased with a 5% increase in slag in the 15G design compared to the previous one, and the final setting decreased by 33.7%. In general, the addition of pozzolans has reduced the interval between the initial and final setting, reducing the difference of 60.5% in the control design to 9.59% in the 10G design. In addition, 5G, 5Z, and 10Z designs with 3.28%, 9.84%, and 19.7% differences compared to the control design at the time of final setting, respectively, have the shortest distance in terms of setting rate with the control design. Increasing the percentage of zeolite and slag pozzolans to more than 10% has led to a decrease of setting time which from this perspective, had a negative effect on the behavior of UHPC.

3.2 Mechanical properties

The trend of increasing compressive strength in the first 2 days of curing for designs containing slag (Fig. 4a), implied a higher initial strength than the control design that is increasing the percentage of pozzolan which had a direct effect on reducing the amount of compressive strength. In the first ½ day of curing, the highest compressive strength belongs to the 5G design, which is 2.74 times higher than the control design. The strength growth rate continued to slow down gradually for the slag-containing designs compared to the control design, and on the second day (first 2 days), the 10G and 15G designs showed lower strength than the control design. This relatively initial fast setting, which has occurred due to the cementitious properties of slag and the increased hydration activity of cementitious and pozzolanic particles, can create a remarkable potential in UHPC and enable rapid repair and temporary applications before ½ day. Zeolite, on the other hand (Fig. 4b), behaved much similar to the control design in UHPC. A much smaller increase in strength observed in the first ½ day (maximum 67.1% increase in the 10Z design). Unlike slag-containing designs, in zeolite-containing designs, the growth trend of compressive strength was still higher than the control design during the first 2 days, and despite the results of these designs approaching the control design at the end of first day, again at 2 days of age, the distance between the results increased. This unique effect of zeolite, which unlike cement, is not hydration related, could be originated from its high porosity and the role of zeolite in internal curing and relatively better hydration of cement particles. In designs containing the two pozzolans (Fig. 4c), zeolite also reduced the impact of slag and thus reduced the hardening process rate. At age of 2 days, significantly increasing the percentage of total pozzolans to 15% has resulted in lower compressive strength than the control design. The 5G10Z design, which also has a higher ratio of zeolite, at this age has resulted in the lowest compressive strength compared to other compositions (13.4% lower than

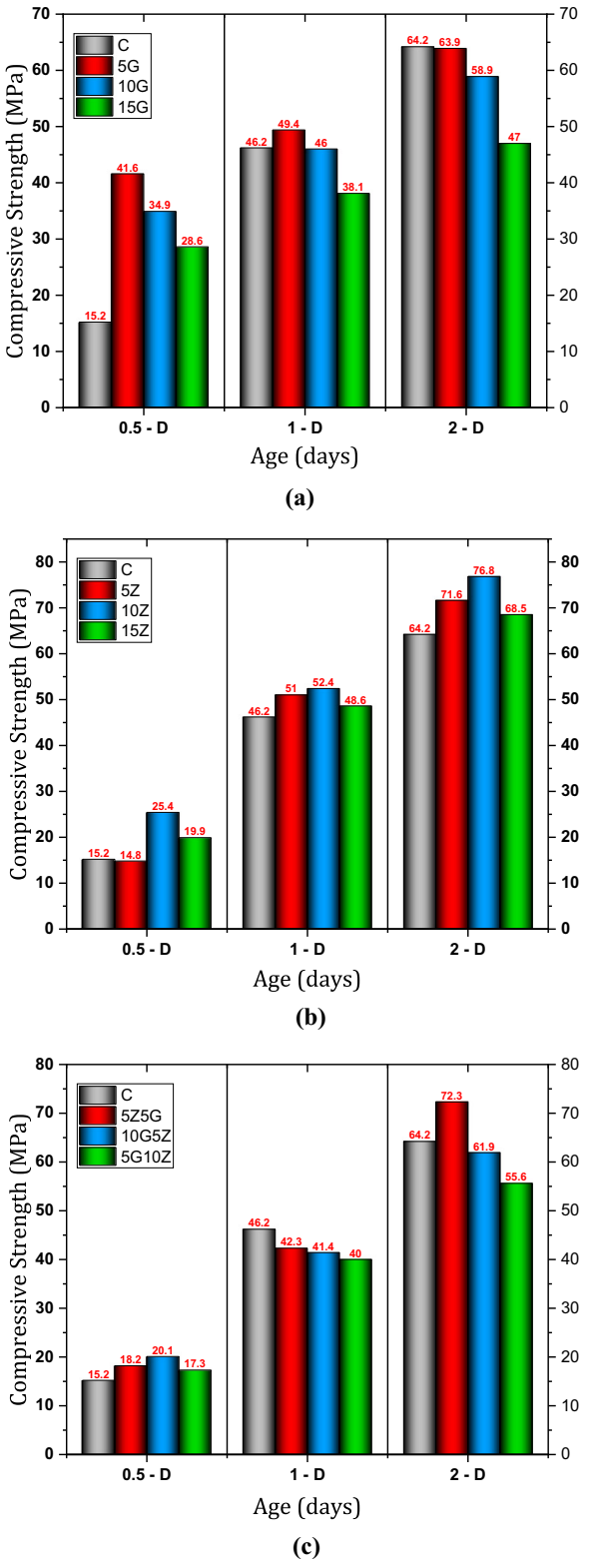

Fig. 4 Comparison of compressive strength of control design at 1/2, 1, and 2 days of curing with **a** designs containing slag pozzolans, **b** designs containing zeolite pozzolans, **c** designs containing slag and zeolite pozzolans simultaneously

the control design). Zeolite seems to have played an influential role in reducing the pozzolanic and cementitious activity of slag.

As shown in Fig. 5, at 90 days, most designs experienced a decrease in compressive strength due to the accelerating agent negative effect. The only exception is the 5Z design, in which the positive impact of 5% zeolite resulted in a 3.1% increase in compressive strength at 90 days compared to the age of 28 days. At different ages, the replacement of slag pozzolans, both individually and collectively, by 15%, led to a reduction in compressive strength compared to the control design in most cases which is supported by other studies (Mounira et al. 2021; Chadli et al. 2020; Tebbal and Rahmouni 2016). However, the 15G, and 15Z designs at the age of 90 days showed a slight increase (1.79% and 4.46%, respectively) due to the pozzolanic effect on the trend of increasing strength. Furthermore, the role of aggregates is undeniable which some studies support the effect of aggregates at higher ages (Tebbal and Rahmouni 2016).

The results of flexural strength (Fig. 6) also show a decrease in values at 90 days compared to the period of 28 days, which is consistent with the results of compressive strength. This reduction in strength, previously attributed to the accelerating effect, is not observed in the 5Z design, and this exception can also be seen in the compressive strength results. The 7 day age of flexural specimens show the maximum amount of 14.3 MPa for 5Z5G mix design. Furthermore, the results as expected are close to 28 day results similar to compressive strength data. The flexural strength results of different designs at the age of 28 days are relatively close to each other. The minimum flexural strength is recorded in the 5G10Z design with 17.3 MPa, and the maximum in the 5Z design is 20 MPa. Very close results in flexural strength may indicate less sensitivity of these results to the effect of pozzolans compared to the results of compressive strength.

3.3 Electrical properties and water absorption

The trend of changes in electrical resistivity in the first 2 days of curing for designs containing slag (Fig. 7a) revealed the positive effect of slag on the improvement of electrical resistivity at the end of ½ day curing. The presence of 5% slag led to an increase 2.07 times the electrical resistivity at this age compared to the control design. As the percentage of slag increased at this age, the electrical resistivity decreased. However, up to 15%, the higher results were recorded compared to the control mix design. At the first day of age, the electrical resistivity of the 5G design was still 153% higher than the control design, but the results of the designs containing 10% and 15% slag were closer to the control design. At 2 days of age, the control design showed a significant increase in electrical resistivity and appeared at least 14.9%

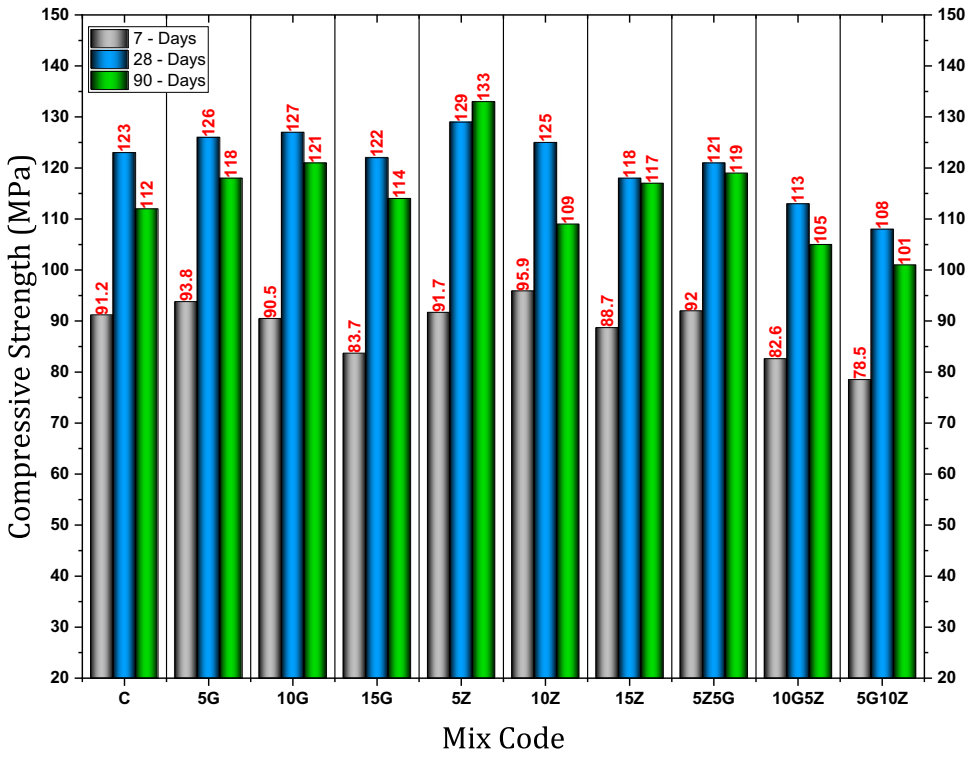

Fig. 5 Compressive strength of different pozzolanic UHPC designs at the ages of 7, 28, and 90 days

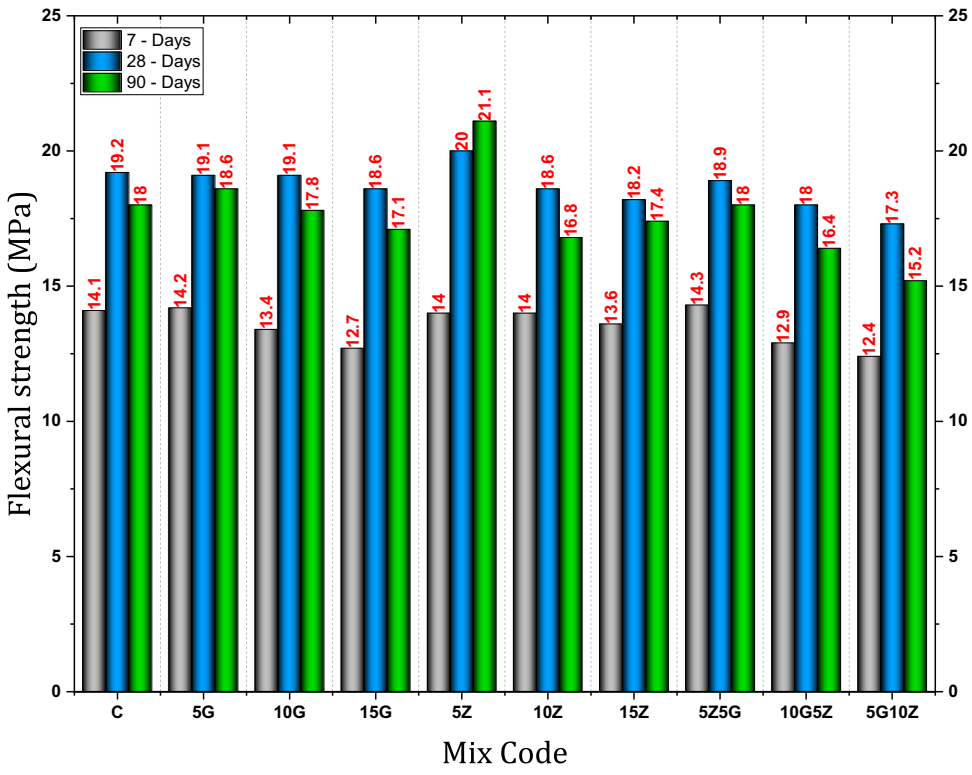

Fig. 6 Flexural strength of different designs at the ages of 7, 28, and 90 days

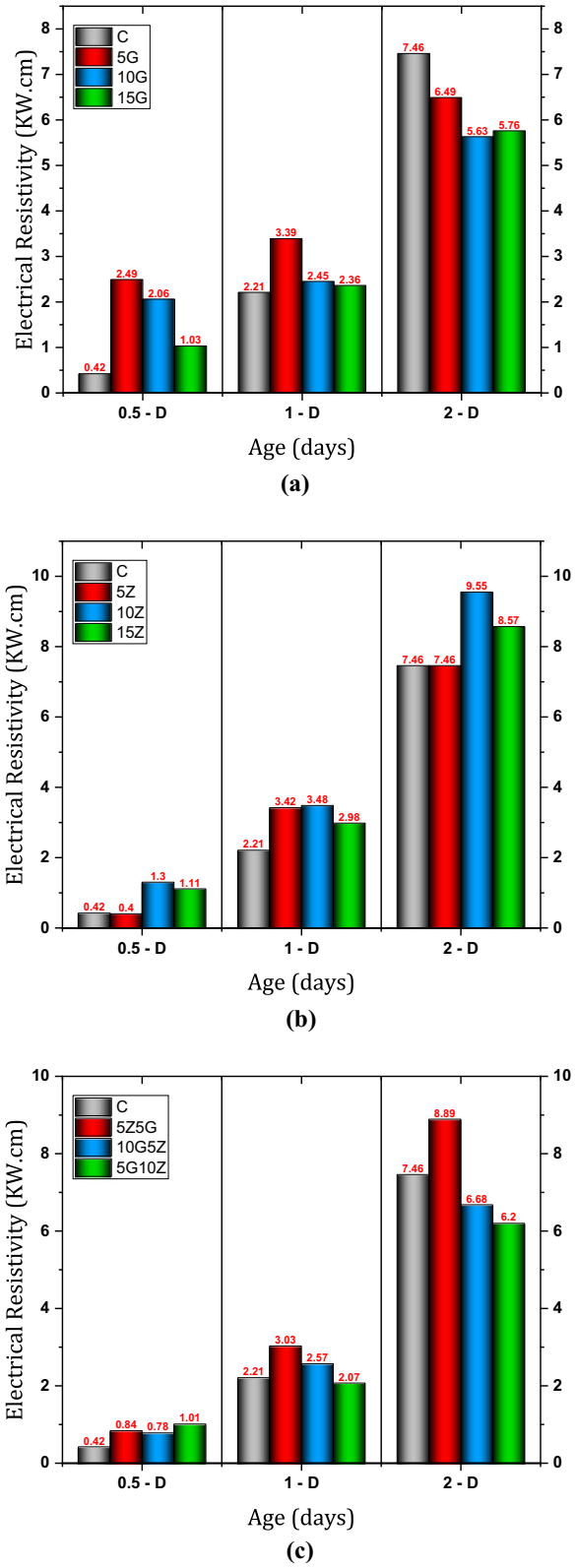

Fig. 7 Comparison of electrical resistivity of control design at 1/2, 1, and 2 days of curing with **a** designs containing slag pozzolans, **b** designs containing zeolite pozzolans, **c** designs containing slag and zeolite pozzolans simultaneously

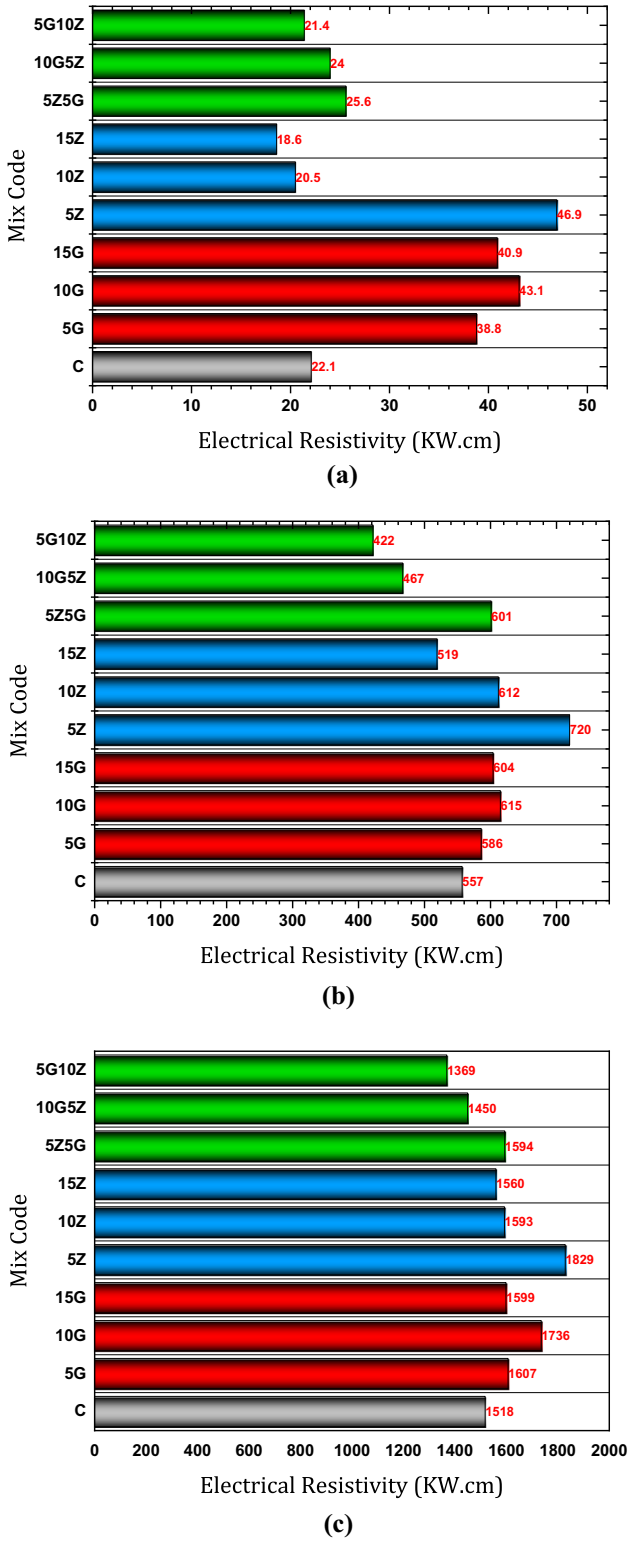

Fig. 8 Electrical resistivity of different pozzolanic UHPC designs at **a** 7 days, **b** 28 days, and **c** 90 days

(compared to the 5G design) higher than other designs. The trend of changes in slag-containing designs reveals the cross-sectional effect, and intense slag activity, especially in the first curing day. In designs containing zeolite (Fig. 7b), the results are closer to the control design. At the end of ½ day, the 5Z design has almost the same results as the control design, and the 10Z and 15Z designs show higher results with a 164% increase over the control design. At the end of the first curing day, the results of zeolite-containing designs became more distant from the control design and closer to each other. The trend of changes in electrical resistivity of these designs changed after 1 day of curing. At the age 2 days, the 5Z design approached the control design again, while the 10Z design was, furthermore, associated with an increase in electrical resistivity. The effect of zeolite probably led to a turning point at the age of 1 day due to the complexities caused by porosity and the pozzolanic effect, which had both negative and positive effects on electrical resistivity.

According to Fig. 8, the sharp increase in electrical resistivity after the age of 7 days is well visible. At the age of 28 days, the minimum increase in electrical resistivity (in the 10G design) compared to the age of 7 days 14.3 times, and at the age of 90 days (5Z). The minimum increase in resistivity compared to the age of 28 days was 2.54 times. These drastic changes, which are significantly different from the compressive strength growth rate, regardless of the mechanical structure, probably occurred due to chemical changes in the cement matrix and the closure of capillary pores with the development of hydration. In addition, at the age of 90 days, all designs containing slag and zeolite pozzolans individually had higher results than the control design, which shows the optimal performance of pozzolans in improving the durability of UHPC. Compositions containing 15% of binary pozzolans showed lower results at 90 days than the control design.

The lowest amount of water absorption, according to the diagram in Fig. 9, belongs to the 5Z design, which is consistent with other results. This composition can be suggested as the optimal one. This result is in good agreement with the results of electrical resistivity and the positive effect of pozzolans, except for the designs of 10G5Z and 5G10Z, which are well-reflected in the results. The reduction of water absorption due to the significant improvement of hydration, which results from the favorite activity of slag and zeolite, seems to be a logical reason for these values.

3.4 Correlation of results

Correlation with coefficients above 85% between the results of compressive strength and flexural strength at 28 and 90 days (Fig. 10) has shown a significant exponential relationship between these two groups of results. The higher

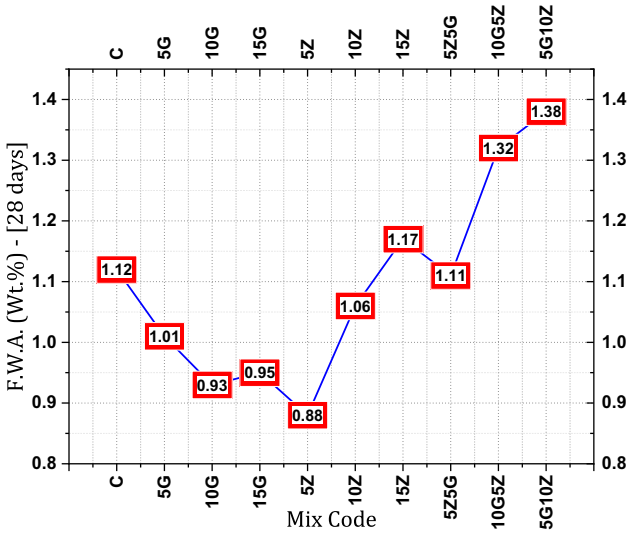

Fig. 9 Percentage by weight of final water absorption of various pozzolanic UHPC designs at 28 days of age

slope of the chart at 90 days can be related to the improvement of flexural strength against compressive strength at this age. In addition, at the age of 90 days, the obtained exponential relationship was more consistent with the experimental results, and the correlation coefficient reached 88%, which shows a stronger connection between the results of compressive and flexural strength at higher ages.

The relationships between compressive strength and electrical resistivity at the ages of 28 and 90 days (Fig. 11) have relatively high correlation coefficients (at least 86.4%). In contrast to the correlation between the results of mechanical tests, at 90 days, the relationship between the results is slightly weaker. This decrease in correlation can be attributed to the difference in the growth of electrical resistivity compared to the compressive strength for the two types of pozzolans.

An excellent linear correlation (with a correlation coefficient of 87.9%) is shown in Fig. 12 between the results of electrical resistivity and final water absorption at the age of 28 days. This linear and inverse relationship has shown the strong dependence of the results of electrical resistivity on the water absorption of the specimens and their subsequent porosity.

3.5 Microstructure

Figure 13 shows the microstructures of two selected compositions, 5Z, and 5G, at different magnifications. Figure 13a shows the abandoned particles of silica fume in the closed cavities of the cement matrix. The high density of matrix and sharp-edge crystals of unhydrated cement particles can be seen in this image. Also shown in Fig. 13b is the multi-growth direction of the C.S.H gel within the cement matrix,

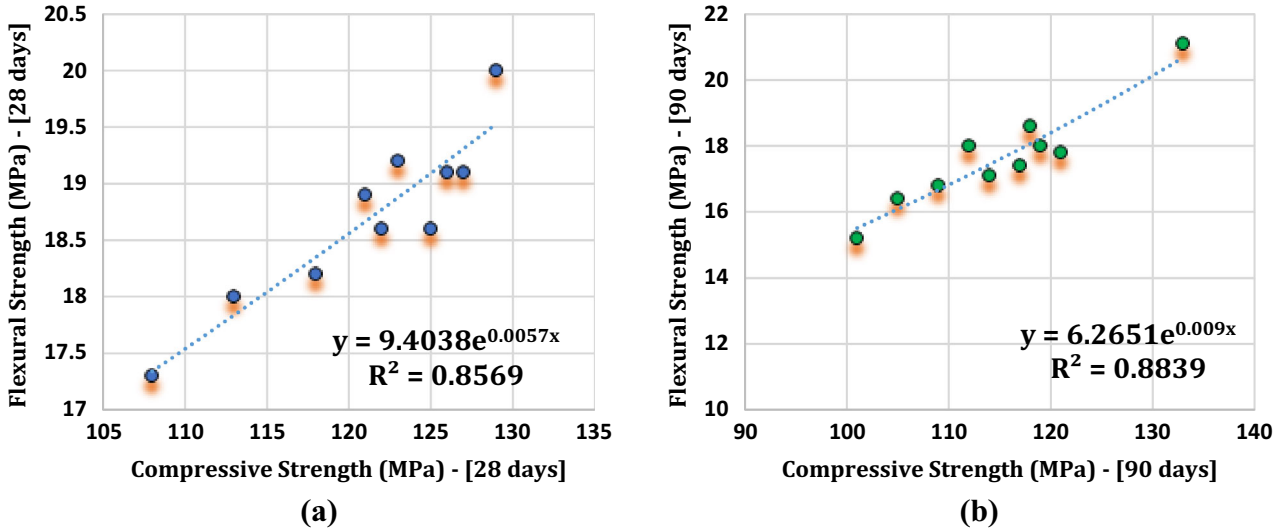

Fig. 10 Correlation between the results of compressive strength and flexural strength at the ages of **a** 28 days and **b** 90 days

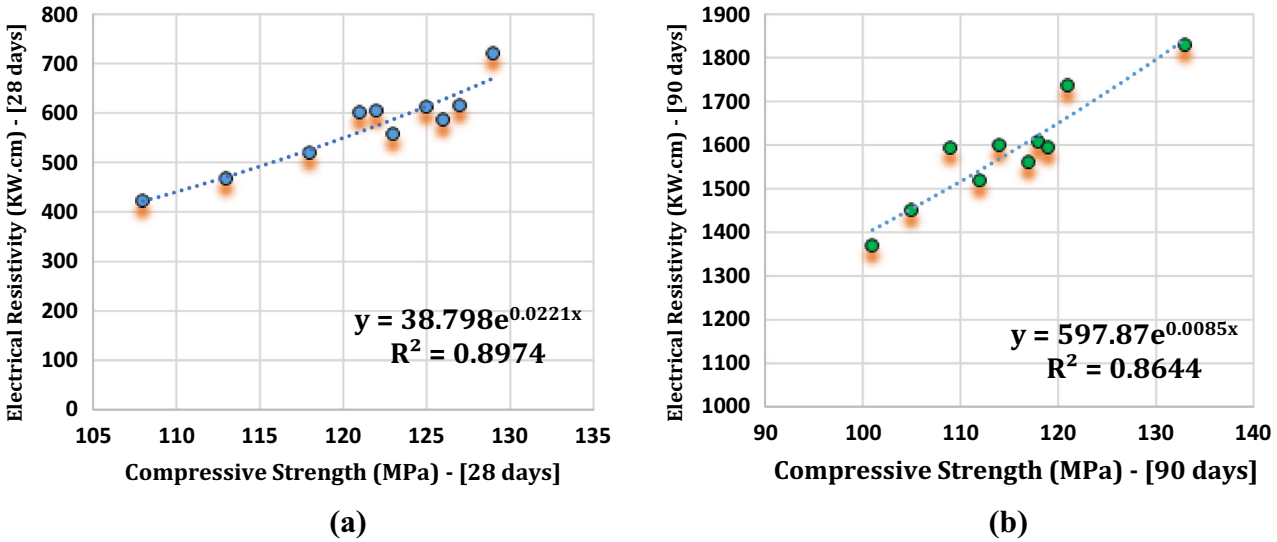

Fig. 11 Correlation between the results of compressive strength and electrical resistivity at the ages of **a** 28 days and **b** 90 days

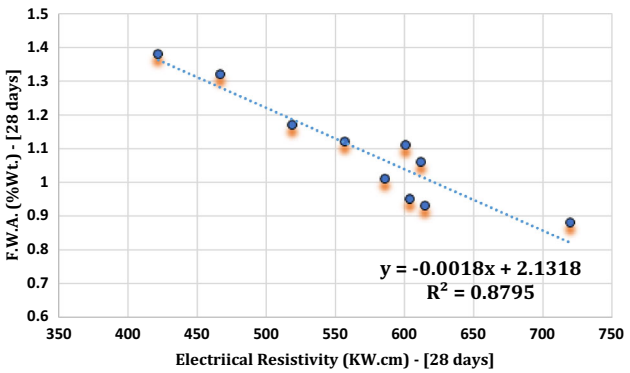

Fig. 12 Correlation between the results of electrical resistivity and water absorption at the age of 28 days

as one of the main reasons for the significant increase in compressive strength and electrical resistivity values, can be considered. Fractured pieces of sand with a lighter color can be detected on the cement matrix in Fig. 13c. Scattered silica fume particles are also detectable in this image, which is less numerous than in Fig. 13a. In this specimen, too, the high degree of packing of the cement matrix due to the development of C.S.H. is visible. In addition, anhydrate cement crystals are observable on the broken surface of concrete, which can be due to the effect of slag on the optimal development of the gel and reducing the number of raw cement crystals. Figure 13d shows development of a different structure of C.S.H. gel and it is shown in Fig. 13b and at the same magnification. The gel mass structures are relatively larger and do not follow a specific orientation.

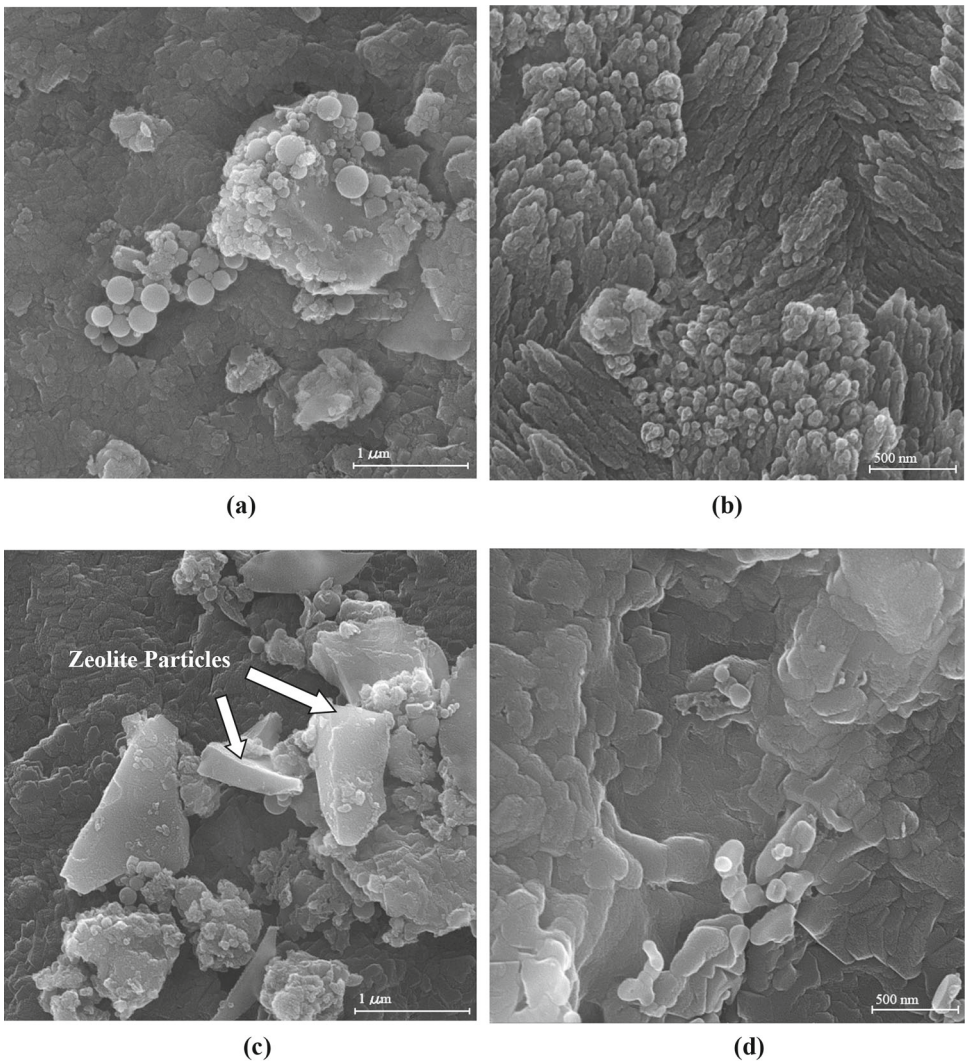

Fig. 13 5Z design microstructure at: **a** 50 kX and **b** 75 kX—5G design at: **c** 50 kX and **d** 75 kX

4 Conclusion

Mix designs of pozzolanic modified UHPCs that investigated in this study with the aim of rapid repair and cold region applications in relatively short periods and time sensitive manners, in addition to optimal performance in the first 2 days, at higher ages also maintain the range of optimal characteristics of UHPCs and efficiency they have been proven for utilization in industry. According to the results obtained and the interpretations provided, the following can be summarized in the conclusion of the study:

- The internal heat evolution of UHPCs containing slag and zeolite was delayed compared to the control design which is a crucial factor for time sensitive projects. Higher temperatures were recorded as a result of the pozzolanic reaction process, in which slag showed more intense activity than zeolite and the highest hydration reaction temperature belonged to designs containing slag. This behavior of slag is useful to control drawbacks such as early cracks during the hardening of UHPC.
- The setting time of the designs containing single zeolite and slag pozzolans, except for the 10G design, was relatively short compared to the control design, and the complex designs with 15% of single pozzolans had a somewhat higher setting time. Depending on the project requirements, each mix design can be ideal for the specifications of that project.
- The growth trend of compressive strength in the first ½ day was intense and unique in the compositions incorporating slag and zeolite as well as the designs containing two pozzolans showed less difference than the control design. These combinations could be beneficial specially for cold and dry climates.
- At the ages of 1 and 2 days, the growth trend of compressive strength for pozzolanic designs decreased, and the control design, in most cases, surpassed the pozzolanic designs.

- At 90 days, the negative accelerating agent effect on compressive strength was noticeable, although the 5Z design, unlike other designs, experienced a slight increase in compressive strength at this age which eliminates the drawback of using accelerating agent. In addition, at the periods of 7 and 28 days, designs containing 15% of pozzolan showed a decrease in compressive strength compared to the control design.
- Severe changes in electrical resistivity of slag-containing designs at early ages, up to 2 days, compared to zeolite and complex designs, showed the effect of slag in blocking capillary pores. This is useful specifically for reinforced elements in a freezing environment.
- The rapid increase in electrical resistivity at the ages of 28 and 90 days for pozzolanic mix designs, regardless of changes in compressive strength, was a prominent result of this study. This enormous rise of ER, ensures drastically long service life of the concrete element.
- A strong mathematical correlation was established at the ages of 28 and 90 days between the results of compressive and flexural strength, and compressive strength and electrical resistivity.
- Microstructural images of the two selected designs revealed highly dense structural matrix, and different behavior of the two pozzolans revealed.

4.1 Scope of the future research

This study is a beginning framework for research projects concerning rapid repairs and cold region applications of UHPC. Using pozzolans to control the fresh state behavior of this concrete in a timely manner and the elimination of drawbacks at the long term, could pave the way for more sophisticated civil engineering projects. More variety of tests including different environments and utilization of chemical admixtures to improve the performance of pozzolans are expected to facilitate industrial applications of engineered UHPCs.

Author contributions AHM supervised the research. BBN conducted the research, wrote the main manuscript text and prepared the figures and tables.

Funding This research did not receive any specific grant from funding agencies in the public, commercial, or not-for-profit sectors.

Data availability The data set analyzed during the current study is available and can be provided upon request.

Declarations

Conflict of interest The authors declare no competing interests.

References

AASHTO TP 95-11 (2011) Standard test method for surface resistivity indication of concrete's ability to resist chloride ion penetration. Aashto

Ahmad I, Shen D, Khan KA, Jan A, Khubaib M, Ahmad T, Nasir H (2022) Effectiveness of limestone powder in controlling the shrinkage behavior of cement based system: a review. Silicon

Ahmadi B, Shekarchi M (2010) Use of natural zeolite as a supplementary cementitious material. Cem Concr Compos. https://doi.org/10.1016/j.cemconcomp.2009.10.006

American Society for Testing and Materials (2008) ASTM C191-08 standard test methods for time of setting of hydraulic cement by vicat needle. Annual Book of ASTM Standards 191-04

An GH, Park JM, Cha SL, Kim JK (2016) Development of a portable device and compensation method for the prediction of the adiabatic temperature rise of concrete. Constr Build Mater. https://doi.org/10.1016/j.conbuildmat.2015.10.143

ASTM C348-21 (2021) Standard test method for flexural strength of hydraulic-cement mortars. ASTM International, 04

ASTM C494 (2013) Standard specification for chemical admixtures for concrete. Annual Book of ASTM Standards, 04

ASTM International (2005) C109/C109M-05. Standard test method for compressive strength of hydraulic cement mortars. Annual Book of ASTM Standards

ASTM International (2017) ASTM C1856/C1856M-17—standard practice for fabricating and testing specimens of ultra-high performance concrete. ASTM International, 04.02

ASTM (2019) ASTM C150/C150M-19a standard specification for Portland cement. Annual Book of ASTM Standards

ASTM (2020) ASTM C1240 standard specification for silica fume used in cementitious mixtures. Annual Book of ASTM Standards

ASTM-C642 (2013) ASTM C642-13 standard test method for density, absorption, and voids in hardened concrete. Annual Book of ASTM Standards, (3)

Bahmani H, Mostofinejad D (2022) Microstructure of ultra-high-performance concrete (UHPC)—a review study. J Build Eng 50:104118

Bajaber MA, Hakeem IY (2021) UHPC evolution, development, and utilization in construction: a review. J Mater Res Technol 10:1058–1074

British Standards Institution (2019) BS EN 12390-3:2019. Testing hardened concrete part 3: compressive strength of test specimens. BSI Standards Publication

Caputo D, Liguori B, Colella C (2008) Some advances in understanding the pozzolanic activity of zeolites: the effect of zeolite structure. Cem Concr Compos. https://doi.org/10.1016/j.cemconcomp.2007.08.004

Chadli M, Tebbal N, Mellas M (2020) Study of the mechanical behavior of a reactive powder concrete containing fibers. In: Proceedings of the 4th international symposium on materials and sustainable development

Chan SYN, Ji X (1999) Comparative study of the initial surface absorption and chloride diffusion of high performance zeolite, silica fume and PFA concretes. Cem Concr Compos. https://doi.org/10.1016/S0958-9465(99)00010-4

Cosoli G, Mobili A, Tittarelli F, Revel GM, Chiariotti P (2020) Electrical resistivity and electrical impedance measurement in mortar and concrete elements: a systematic review. Appl Sci (switzerland). https://doi.org/10.3390/app10249152

Du J, Meng W, Khayat KH, Bao Y, Guo P, Lyu Z, Abu-obeidah A, Nassif H, Wang H (2021) New development of ultra-high-performance concrete (UHPC). Compos B Eng 224:109220

Ghasemzadeh Mosavinejad SH, Langaroudi MAM, Barandoust J, Ghanizadeh A (2020) Electrical and microstructural analysis of UHPC

containing short PVA fibers. Constr Build Mater. https://doi.org/10.1016/j.conbuildmat.2019.117448
Gholhaki M, Kheyroddin A, Hajforoush M, Kazemi M (2018) An investigation on the fresh and hardened properties of self-compacting concrete incorporating magnetic water with various pozzolanic materials. Constr Build Mater. https://doi.org/10.1016/j.conbuildmat.2017.09.135
Gorzelańczyk T, Hoła J (2011) Pore structure of self-compacting concretes made using different superplasticizers. Arch Civ Mech Eng. https://doi.org/10.1016/s1644-9665(12)60104-6
Hajforoush M, Madandoust R, Kazemi M (2019) Effects of simultaneous utilization of natural zeolite and magnetic water on engineering properties of self-compacting concrete. Asian J Civ Eng 20(2):289–300. https://doi.org/10.1007/s42107-018-00106-w
Jan A, Pu Z, Khan KA, Ahmad I, Khan I (2022) Effect of glass fibers on the mechanical behavior as well as energy absorption capacity and toughness indices of concrete bridge decks. SILICON. https://doi.org/10.1007/s12633-021-01026-2
Kim H, Koh T, Pyo S (2016) Enhancing flowability and sustainability of ultra high performance concrete incorporating high replacement levels of industrial slags. Constr Build Mater. https://doi.org/10.1016/j.conbuildmat.2016.06.134
Li J, Wu Z, Shi C, Yuan Q, Zhang Z (2020) Durability of ultra-high performance concrete—a review. Constr Build Mater 255:119296
Liu Z, El-Tawil S, Hansen W, Wang F (2018) Effect of slag cement on the properties of ultra-high performance concrete. Constr Build Mater. https://doi.org/10.1016/j.conbuildmat.2018.09.173
Mansoori A, Mohtasham Moein M, Mohseni E (2020) Effect of micro silica on fiber-reinforced self-compacting composites containing ceramic waste. J Compos Mater. https://doi.org/10.1177/0021998320944570
Moein MM, Soliman A (2022) Predicting the compressive strength of alkali-activated concrete using various data mining methods. In: Canadian society of civil engineering annual conference. Springer Nature, Singapore, pp 317–326
Moein MM, Mousavi SY, Madandoust R, Naser Saeid HNS (2019) The impact resistance of steel fiber reinforcement concrete under different curing conditions: experimental and statistical analysis. J Civ Environ Eng 49(94):109–121
Moein MM, Saradar A, Rahmati K, Hatami Shirkouh A, Sadrinejad I, Aramali V, Karakouzian M (2022) Investigation of impact resistance of high-strength portland cement concrete containing steel fibers. Cem Mater High Perform Concr 15(20):1–30. https://doi.org/10.3390/ma15207157
Moein MM, Saradar A, Rahmati K, Ghasemzadeh Mousavinejad SH, Bristow J, Aramali V, Karakouzian M (2023a) Predictive models for concrete properties using machine learning and deep learning approaches: a review. J Build Eng. https://doi.org/10.1016/j.jobe.2022.105444
Moein MM, Saradar A, Rahmati K, Rezakhani Y, Ashkan SA, Karakouzian M (2023b) Reliability analysis and experimental investigation of impact resistance of concrete reinforced with polyolefin fiber in different shapes, lengths, and doses. J Build Eng. https://doi.org/10.1016/j.jobe.2023.106262
Mosavinejad HG, Saradar A, Tahmouresi B (2018) Hoop stress-strain in fiber-reinforced cementitious composite thin-walled cylindrical shells. J Mater Civ Eng 30(10):1–12. https://doi.org/10.1061/(ASCE)MT.1943-5533.0002428
Mounira C, Nadia T, Mekki M (2021) Study of mechanical and elastic properties of reactive powder concrete. Alger J Eng Res 5:11–17
Pezeshkian M, Delnavaz A, Delnavaz M (2020) Effect of natural zeolite on mechanical properties and autogenous shrinkage of ultrahigh-performance concrete. J Mater Civ Eng. https://doi.org/10.1061/(asce)mt.1943-5533.0002968
Pezeshkian M, Delnavaz A, Delnavaz M (2021) Development of UHPC mixtures using natural zeolite and glass sand as replacements of silica fume and quartz sand. Eur J Environ Civ Eng. https://doi.org/10.1080/19648189.2019.1610074
Poon CS, Lam L, Kou SC, Lin ZS (1999) A study on the hydration rate of natural zeolite blended cement pastes. Constr Build Mater. https://doi.org/10.1016/S0950-0618(99)00048-3
Rahmati K, Saradar A, Mohtasham Moein M, Sardrinejad I, Bristow J, Yavari A, Karakouzian M (2022) Evaluation of engineered cementitious composites (ECC) containing polyvinyl alcohol (PVA) fibers under compressive, direct tensile, and drop-weight test. Multiscale Multidiscip Model Exp Design. https://doi.org/10.1007/s41939-022-00135-8
Sadrmomtazi A, Tahmouresi B, Saradar A (2018) Effects of silica fume on mechanical strength and microstructure of basalt fiber reinforced cementitious composites (BFRCC). Constr Build Mater. https://doi.org/10.1016/j.conbuildmat.2017.11.159
Sadrmomtazi A, Noorollahi Z, Tahmouresi B, Saradar A (2019) Effects of hauling time on self-consolidating mortars containing metakaolin and natural zeolite. Constr Build Mater. https://doi.org/10.1016/j.conbuildmat.2019.06.037
Saradar A, Tahmouresi B, Mohseni E, Shadmani A (2018) Restrained shrinkage cracking of fiber-reinforced high-strength concrete. Fibers. https://doi.org/10.3390/fib6010012
Saradar A, Nemati P, Paskiabi AS, Moein MM, Moez H, Vishki EH (2020) Prediction of mechanical properties of lightweight basalt fiber reinforced concrete containing silica fume and fly ash: experimental and numerical assessment. J Build Eng. https://doi.org/10.1016/j.jobe.2020.101732
Sbia LA, Peyvandi A, Harsini I, Lu J, Abideen SU, Weerasiri RR, Balachandra AM, Soroushian P (2017) Study on field thermal curing of ultra-high-performance concrete employing heat of hydration. ACI Mater J. https://doi.org/10.14359/51689677
Sengul O (2012) Factors affecting the electrical resistivity of concrete. RILEM Bookseries, p 6. https://doi.org/10.1007/978-94-007-0723-8_38
Shadmani A, Tahmouresi B, Saradar A, Mohseni E (2018) Durability and microstructure properties of SBR-modified concrete containing recycled asphalt pavement. Constr Build Mater. https://doi.org/10.1016/j.conbuildmat.2018.07.080
Sharma R, Jang JG, Bansal PP (2022) A comprehensive review on effects of mineral admixtures and fibers on engineering properties of ultra-high-performance concrete. J Build Eng 45:10331
Shaukat AJ, Feng H, Khitab A, Jan A (2020) Effect of admixtures on mechanical properties of cementitious mortar. Civ Eng J (iran). https://doi.org/10.28991/cej-2020-03091610
Shi C, Wu Z, Xiao J, Wang D, Huang Z, Fang Z (2015) A review on ultra high performance concrete: part I. Raw materials and mixture design. Constr Build Mater 101:741–751
Soliman AM, Nehdi ML (2013) Effect of partially hydrated cementitious materials and superabsorbent polymer on early-age shrinkage of UHPC. Constr Build Mater. https://doi.org/10.1016/j.conbuildmat.2012.12.008
Stein B, Kramer B, Pyle T, Shatnawi S (2010) Rapid strength concrete for rehabilitation and improvement of pavements. In: First international conference on pavement preservation, pp 411–426
Tahmouresi B, Nemati P, Asadi MA, Saradar A, Mohtasham Moein M (2021) Mechanical strength and microstructure of engineered cementitious composites: a new configuration for direct tensile strength, experimental and numerical analysis. Constr Build Mater. https://doi.org/10.1016/j.conbuildmat.2020.121361
Tebbal N, Rahmouni ZEA (2016) Influence of local sand on the physicomechanical comportment and durability of high performance concrete. Adv Civ Eng. https://doi.org/10.1155/2016/3897064
United States Department of Transportation (2002) FHWA MCL Project # 9902/use of fast-setting hydraulic cement concrete for interstate concrete pavement rehabilitation

Viviani M, Lanzoni L, Savino V, Tarantino AM (2022) An auto-calibrating semi-adiabatic calorimetric methodology for strength prediction and quality control of ordinary and ultra-high-performance concretes. Materials. https://doi.org/10.3390/ma15010087

Wang D, Shi C, Wu Z, Xiao J, Huang Z, Fang Z (2015) A review on ultra high performance concrete: Part II. Hydration, microstructure and properties. Constr Build Mater 96:368–377

Wang X, Yu R, Song Q, Shui Z, Liu Z, Wu S, Hou D (2019) Optimized design of ultra-high performance concrete (UHPC) with a high wet packing density. Cem Concr Res. https://doi.org/10.1016/j.cemconres.2019.105921

Wang X, Wu D, Zhang J, Yu R, Hou D, Shui Z (2021) Design of sustainable ultra-high performance concrete: a review. Constr Build Mater 307:124643

Wei X, Xiao L (2013) Electrical resistivity monitoring and characterisation of early age concrete. Mag Concr Res. https://doi.org/10.1680/macr.12.00127

Woo HM, Kim CY, Yeon JH (2018) Heat of hydration and mechanical properties of mass concrete with high-volume GGBFS replacements. J Therm Anal Calorim. https://doi.org/10.1007/s10973-017-6914-z

Xiao R, Deng ZC, Shen C (2014) Properties of ultra high performance concrete containing superfine cement and without silica fume. J Adv Concr Technol. https://doi.org/10.3151/jact.12.73

Yalçınkaya Ç, Çopuroğlu O (2021) Hydration heat, strength and microstructure characteristics of UHPC containing blast furnace slag. J Build Eng. https://doi.org/10.1016/j.jobe.2020.101915

Yazici H, Yardimci MY, Yiğiter H, Aydin S, Türkel S (2010) Mechanical properties of reactive powder concrete containing high volumes of ground granulated blast furnace slag. Cem Concr Compos. https://doi.org/10.1016/j.cemconcomp.2010.07.005

Yu R, Spiesz P, Brouwers HJH (2014) Mix design and properties assessment of ultra-high performance fibre reinforced concrete (UHPFRC). Cem Concr Res. https://doi.org/10.1016/j.cemconres.2013.11.002